Available online at www.sciencedirect.com
ScienceDirect
Colloids and Surfaces A: Physicochem. Eng. Aspects 299 (2007) 109–116
COLLOIDS AND SURFACES A
www.elsevier.com/locate/colsurfa

Automatic measurement of surface tension from noisy images using a component labeling method

Yi Y. Zuo [a], Chau Do [b], A. Wilhelm Neumann [a,*]

[a] Department of Mechanical and Industrial Engineering, University of Toronto, 5 King's College Road, Toronto, Ont. M5S 3G8, Canada
[b] Department of Systems Design Engineering, University of Waterloo, 200 University Avenue West, Waterloo, Ont. N2L 3G1, Canada

Received 20 July 2006; received in revised form 29 October 2006; accepted 14 November 2006
Available online 19 November 2006

Abstract

Automatic surface tension measurement of turbid liquids using a bubble method (e.g., pendant/captive bubble) or interfacial tension measurement of some liquid–liquid systems necessitates an image analysis scheme robust against noise. Measuring the surface tension of lung surfactant–polymer systems using the combination of axisymmetric drop shape analysis (ADSA) and a captive bubble is such an example. We have recently developed a sophisticated image analysis scheme featuring the combination of the Canny edge detector and a novel edge smoothing technique called axisymmetric liquid fluid interfaces-smoothing (ALFI-S). The Canny edge detector is highly noise-resistant and ALFI-S is efficient in further removing noise close to the bubble profile (i.e., adhering noise). However, the procedure of eliminating noise far away from the bubble profile (i.e., isolated noise) is still not satisfactory in the previous scheme. Here a component labeling method is developed to automatically remove isolated noise. Component labeling refers to the process of detecting connected objects in a digital image. Once labeling is completed, information, such as area, location and pixel intensity, of these separate objects can be obtained. Hence, component labeling can be used as a region-based segmentation technique that is capable of differentiating the bubble and the isolated noise. The new component labeling-based noise reduction method is used to analyze captive bubble images with different amounts of noise. It is found that with the help of the labeling procedure smooth edges can be detected with a simple set of user-specified parameters even from images with extensive noise. Combined with the previous image analysis scheme, the component labeling method significantly improves the effectiveness and reliability of ADSA in automatically measuring surface tension from noisy images.

Keywords: Axisymmetric drop shape analysis (ADSA); Surface tension measurement; Component labeling; Image analysis; Biofluids

1. Introduction

Surface tension measurement plays an important role in a variety of scientific and industrial fields, such as biomedical engineering, pharmaceutical industry, petroleum refining, polymer testing, printing industry, semiconductor industry, cosmetics, paper industry, food industry, textiles and adhesives [1,2]. Among the commonly used methods, drop shape methods offer a number of advantages as they require less liquid samples, are applicable to both air–liquid and liquid–liquid interfaces, and are versatile and applicable to various situations, including extreme temperature and pressure [3].

Axisymmetric drop shape analysis (ADSA) is a surface tension measurement methodology based on the shape of drops or bubbles. ADSA was first developed in the authors' laboratory in the 1980s [4]. In the last two decades, the original algorithm has been significantly improved [5,6]. So far, ADSA has been used worldwide by a number of laboratories/companies for a variety of studies. Due to its accuracy, simplicity, and versatility, ASDA has been evaluated as a standard method for surface tension measurement [7].

A recent focal point is the use of ADSA to study biofluids, e.g., lung surfactant (a phospholipid–protein complex in the mammalian lungs that reduces the alveolar surface tension and maintains alveoli against collapse) (for reviews, see [8,9]). ADSA is found to be very suitable for such studies due to the following facts: (1) it only requires an amount of liquid samples as little as a few microliters, which minimizes the cost of experimental materials. (2) ADSA is capable of simultaneously

* Corresponding author. Tel.: +1 416 978 1270; fax: +1 416 978 7753.
E-mail address: neumann@mie.utoronto.ca (A.W. Neumann).

0927-7757/$ – see front matter © 2006 Elsevier B.V. All rights reserved.
doi:10.1016/j.colsurfa.2006.11.027

measuring surface tension and surface area, thus allowing for recording surface tension–area isotherms. This feature makes ADSA a micro-film balance, an intriguing alternative to the traditional film balance for studying insoluble films. (3) ADSA allows measurement of dynamic surface tension. Therefore, it is possible to investigate the highly dynamic properties of biofluids, e.g., rapid adsorption and dynamic cycling of lung surfactant films at the physiologically relevant rate. (4) ADSA is capable of measuring very low surface tension (less than 1 mJ/m^2), occurring in lung surfactant systems. (5) ADSA is highly automated and hence its operation is less dependent on the skill of the operator.

In spite of these desirable traits one big challenge remains when ADSA is used to study a liquid–liquid system with the outer liquid being turbid, or certain air–liquid systems with a turbid liquid, such as the captive bubble method in studying lung surfactant. This is due to the fact that the turbid liquid introduces significant optical noise into the drop/bubble images, which makes effective and automatic image analysis difficult to perform. Although a pendant drop in air is not affected by this constraint, the use of a bubble method is sometimes a necessity, e.g., for the measurement of very low surface tension of lung surfactant systems, as detailed later. As an illustration, Fig. 1 shows a sample image of a captive bubble in the mixture of 0.5 mg/mL bovine lipid extract surfactant (BLES) and 50 mg/mL polyethylene glycol (PEG). It is noted that apart from the bubble numerous small particles are randomly distributed throughout the image. These particles are large phospholipid aggregates flocculated by the addition of PEG (likely due to a polymer-induced depletion–attraction mechanism [10,11]). Presence of these large aggregates significantly increases the optical noise of the image, thus making it difficult to extract a smooth bubble profile. It has been established that the quality of the detected edge is the main accuracy-limiting factor of ADSA [12]. Therefore, the accuracy of surface tension measurement from noisy images of turbid liquids can be significantly decreased.

We have recently developed a sophisticated image analysis scheme for measuring surface tension from a noisy image [13]. In that method, the Canny edge detector is first used to extract the bubble profile and any remaining noise due to insufficient noise suppression in the Canny is further removed using a novel two-step noise reduction system. As shown in Fig. 1, noise in a captive bubble image can be differentiated into two categories based on its relative distance to the main bubble profile: isolated noise (i.e., the noise far away from the main bubble profile) and adhering noise (i.e., the noise close to the main bubble profile). First, the isolated noise is removed by measuring edge cohesion: the binary image after edge detection (edge: black; background: white) is raster scanned from left to right and top to bottom. Any assumed edge pixel away from the main profile by 50 pixels (accounting for approximately 0.5 mm) is eliminated as isolated noise [13]. Subsequently, the adhering noise is removed by a novel edge smoothing technique, axisymmetric liquid fluid interfaces-smoothing (ALFI-S) [13]. It was found that the new image analysis scheme is capable of analyzing images in a variety of optical conditions, including images with extensive noise, poor contrast, or non-uniform background lighting [13]. Since the accuracy of ADSA is limited by the quality of the detected edge, the improvement in image analysis has significantly promoted the accuracy of ADSA on measuring surface tension of turbid liquids, such as lung surfactant–polymer systems [13,14].

In the procedure of removing isolated noise, although plausible in principle, implementation of the cohesion algorithm is not an easy task in practice due to the difficulty in identifying the bubble profile a priori through automatic image analysis. Ideally, the pixels representing the main bubble profile after edge detec-

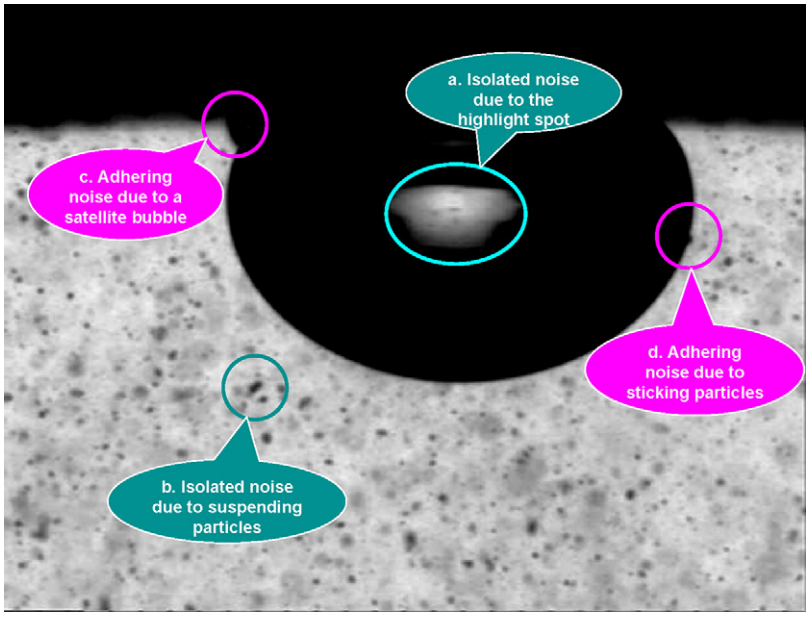

Fig. 1. A sample image showing typical noise in a captive bubble image. The liquid is a mixture of 0.5 mg/mL BLES and 50 mg/mL PEG. There are two categories of noise: (1) isolated noise due to the central highlight spot (a) and due to suspending particles (b); (2) adhering noise due to satellite bubbles (c) and due to adhering particles (d).

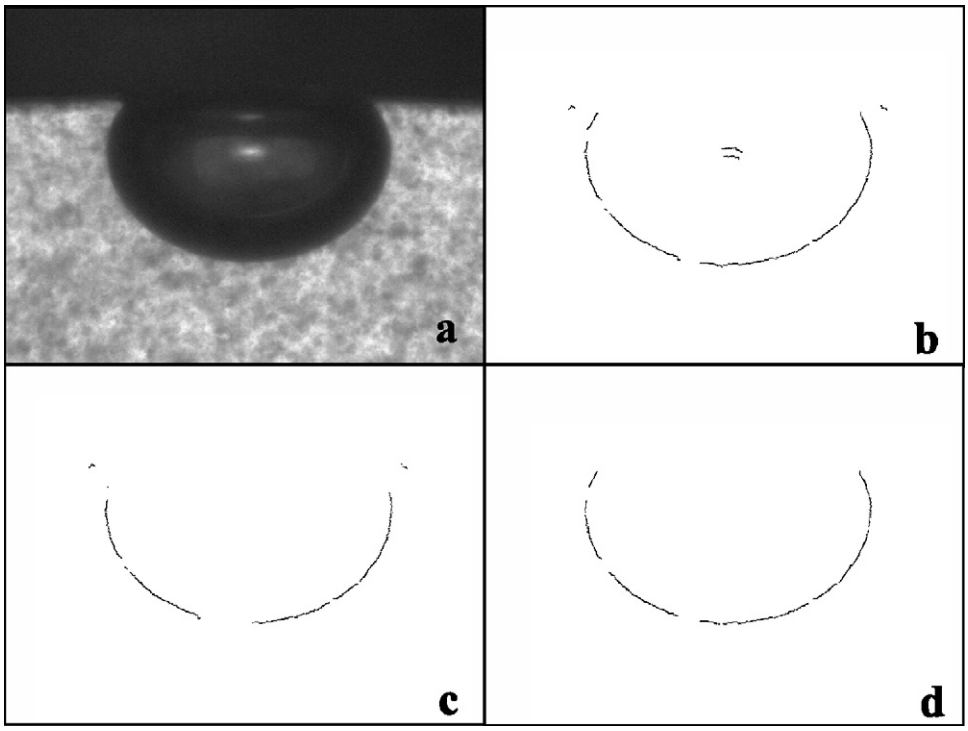

Fig. 2. Illustration of the failure of isolated noise reduction by measuring edge cohesion. (a) An out-of-focus image of a captive bubble in 0.5 mg/mL BLES; (b) Canny detected edge. It is noted that the edge consists of a number of discontinuous segments; (c) edge after "removing" isolated noise by measuring cohesion. It is found that the isolated noise remains but the real edges close to the ceiling are erroneously removed. (d) The smoothed edge using the component labeling-based method developed here. Note that the isolated noise has been effectively removed and a more complete edge is obtained.

tion should be connected and constitute a group that contains many more pixels than the other groups representing the isolated noise. However, this is not the case of most noisy images. For most cases, especially for images lacking in contrast (see Fig. 2(a) for an example), the edge pixels after edge detection is not connected but usually consists of numerous small segments (Fig. 2(b)). The number of connected pixels in each segment and the break between two adjacent segments are random in each image and different from image to image. There is a high possibility that sometimes the pixels in an edge segment are fewer than those in an isolated noise group. This makes it sometimes impossible for the computer system to differentiate the bubble profile by simply measuring edge cohesion and hence causes a difficulty in removing isolated noise in the post-edge detection stage. If isolated noise is erroneously identified as part of the bubble profile, the real edge will be in danger of being removed subsequently. As shown in Fig. 2(c), after measuring cohesion, the isolated noise remains but the real edges close to the ceiling are erroneously removed. It has been established that the edges close to the three-phase contact line of a sessile drop/captive bubble weigh the most in the determination of surface tension [6,12,13]. Hence, the failure in removing isolated noise may cause major errors in the surface tension measurement.

The above difficulties have provoked new thinking on removing isolated noise in the pre-edge detection stage, i.e., the raw image. As show in Fig. 1, a typical captive bubble image features a bubble located in the center of the image, resting against the ceiling and surrounded by aqueous suspension. The bubble accounts for a considerable portion of the image and shows remarkable uniformity of lower intensity than the background. The dominant area and the prominent contrast of the bubble against the background allow for easy localization of the bubble in the raw image and thus permit an alternative way in detecting and removing the isolated noise before edge detection.

In this paper, a component labeling-based region detection technique is developed to remove isolated noise before conducting edge detection. Different images of captive bubbles in water and in mixtures of lung surfactant and polymer are studied to illustrate the effectiveness of the new method. It will be shown that the component labeling method is fully automatic and robust against isolated noise. In conjunction with the Canny edge detector and ALFI-S, the component-labeling method will further strengthen the reliability of ADSA in analyzing noisy images, thus allowing for accurate and automatic surface tension measurement of biofluids and other turbid liquids.

2. Component labeling-based reduction of isolated noise

2.1. Component labeling

Component labeling refers to the process of detecting connected objects in a digital image [15]. A connected component in a digital image refers to a set of pixels in which each pixel is connected to all others [15]. In a 2D image, the connectivity is usually defined by four- or eight-way adjacency. The former only considers the non-diagonal neighbors, while the latter considers all eight possible neighbors of a pixel [15]. Finding connected components in a binary image is one of the most fundamental

operations in computer vision and pattern recognition. Its applications cover a broad range of scientific and industrial fields, such as medical image processing, remote sensing, volume visualization, and character recognition [16]. After component labeling, a binary image is converted into a symbolic image in which each connected component is assigned a unique label [16].

Due to the importance in computer vision and pattern recognition, a large number of algorithms have been developed for component labeling [17–24]. Most of these methods are improved or modified from the classical sequential labeling algorithm proposed by Rosenfeld and Pfaltz [25], in which labeling is performed by two subsequent raster-scans of a binary image. In the first scan a temporary label is assigned to each foreground pixel based on the values of its neighbors (in the sense of four- or eight-connectivity) that have already been visited. When a foreground pixel with its neighbors carrying different labels is found, the labels associated with the pixels in the neighborhood are registered as being equivalent. The second scan replaces each temporary label by the identifier of its corresponding equivalence class. After labeling, the characteristics of each component, such as area, position, orientation and boundary rectangle, can be readily determined. Details of the component labeling algorithm can be found in Refs. [25–27].

2.2. *Development of algorithm: component labeling-based reduction of isolated noise*

In some sense, component labeling is a region-based binary image segmentation technique [27]. During component labeling, each image pixel is examined in the context of its neighbors and a region is grown by addition of new pixels if they are connected. Compared with contour-based segmentation methods (in which a region is identified by first determining its boundary pixels), the region-based methods are relatively insensitive to shape degradation and noise since these methods rely on the entire set of the interior region pixels [27]. Hence, it is possible and desirable to use component labeling for the purpose of noise (especially isolated noise) reduction.

The component labeling-based noise reduction method developed here consists of three steps. First, the original grayscale image is converted into a binary image (black-and-white) using Otsu's thresholding [28]. Second, a modified two-pass sequential labeling process is performed on the binary image. In the first pass, the image is raster scanned and connected pixels are temporarily labeled to be one component. In the second pass, regions connected to each other but with different labels are merged into one component and all components are re-labeled correspondingly. After this step, information on the number of components, area (i.e., number of pixels), location (i.e., coordinates of pixels) and color (i.e., black or white, indicating foreground or background pixels) of each component, is recorded. Also in the second pass of the component labeling, the detected components are ranked in a descending order based on their areas. The components with the first and the second largest areas usually represent the background and the primary foreground object. The other components with much smaller areas represent the noise. After localizing the main object and the noise (i.e., knowing the coordinates of these components), finally, the noise can be safely removed. To do so, in the original grayscale image the intensities of the pixels in the noise components are replaced by the average intensity of their background neighbors, to provide a smoother transition from the regions of the original isolated noise to the background. This action is similar to the application of low-pass filtering to the background of the image [15,16].

It is noteworthy that although thresholding is used as an intermediate step in component labeling, it does not decrease the accuracy of the subsequent surface tension measurement. (It has been found previously that compared with gradient edge operators the use of thresholding to segment drop/bubble profiles degrades the accuracy of surface tension measurement [13,14].) This is due to the fact that thresholding is used here only to facilitate the subsequent component labeling procedure rather than to segment the drop/bubble profile. The labeling procedure only collects the information on the localization of the main object and the isolated noise in an image. Therefore, the grayscale image after component labeling still keeps the original drop/bubble contour except for reduced isolated noise. The detection of the drop/bubble profile still relies on the subsequent Canny edge detector taking advantage of its high accuracy in edge detection.

The flowchart of the entire image analysis scheme used in ADSA, including the component labeling-based noise reduction module developed here, is shown in Fig. 3.

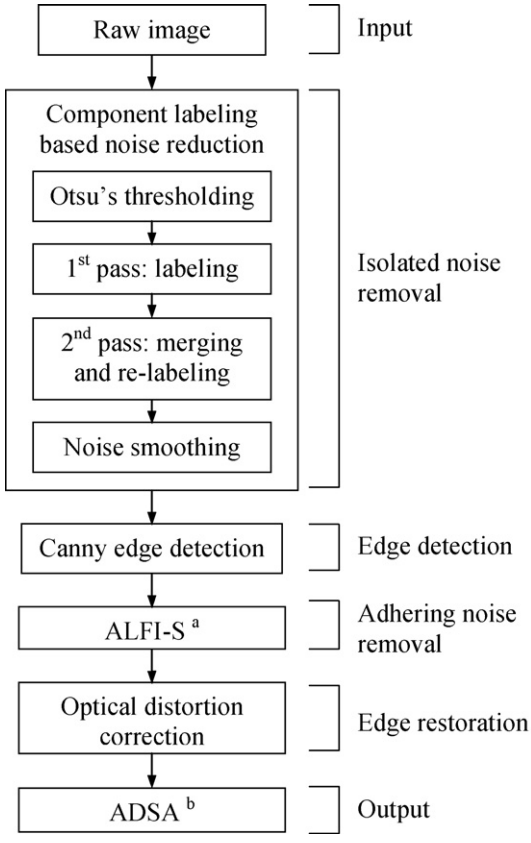

Fig. 3. Flowchart of the image analysis scheme used in ADSA. (a) Axisymmetric liquid fluid interfaces-smoothing; (b) axisymmetric drop shape analysis.

3. Experimental methods

A mixture of bovine lipid extract surfactant (BLES) and polyethylene glycol (PEG) was tested as a representative turbid biofluid. BLES (BLES Biochemicals Inc., London, Ont., Canada) is a clinically used lung surfactant and is commercially available. It was prepared from bovine natural lung surfactant obtained by bronchopulmonary lavage with organic extraction. BLES contains about 98% phospholipids and 2% proteins. BLES was stored frozen in sterilized vials with an initial concentration of 27 mg/mL. It was diluted to 0.5 mg/mL using 0.6% saline with 1.5 mM $CaCl_2$ on the day of experiment. PEG, average molecular weight 10 kDa, was purchased from Sigma Chemical Co. (St. Louis, MO) and used without further purification. PEG at a concentration of 50 mg/mL was mixed with the dilute BLES suspension. It is known that PEG at such a concentration is able to induce large phospholipid aggregates due to a depletion–attraction mechanism [10,11]. These large aggregates significantly increase the chaos of an image.

The captive bubble method [29] was used here for surface tension measurement. Compared with the traditional methods, such as pendant drop and pulsating bubble, the captive bubble method offers a leakage-proof experimental environment, a necessity in studying very low surface tensions of biofluids [9,29]. Film leakage is driven by thermodynamics: a film formed at an air–water interface spreads onto a solid support that contacts the film if the surface tension of the film is lower than that of the solid surface. For Teflon, this limiting surface tension is around 15–18 mJ/m^2. Due to the loss of film material from the air–water interface, film leakage makes the surface tension measurement essentially meaningless. The captive bubble method employs a hydrophilic ceiling that retains a thin aqueous wetting film that separates a bubble from contact with any solid support, thus eliminating all possible pathways for film leakage [29]. Consequently, the captive bubble method is capable of covering a low surface tension range, which makes it an ideal alternative to the traditional methods for surface tension measurement. Detailed setup and protocol of the captive bubble experiments can be found elsewhere [9,13]. All measurements were conducted at 37 °C.

4. Results and discussion

4.1. A captive bubble image with a clean background

To illustrate the performance of the component labeling method, it was first used to study an image with a clean background. Fig. 4(a) shows an image (resolution 376 × 640) of a captive bubble in distilled water. The ceiling of the captive

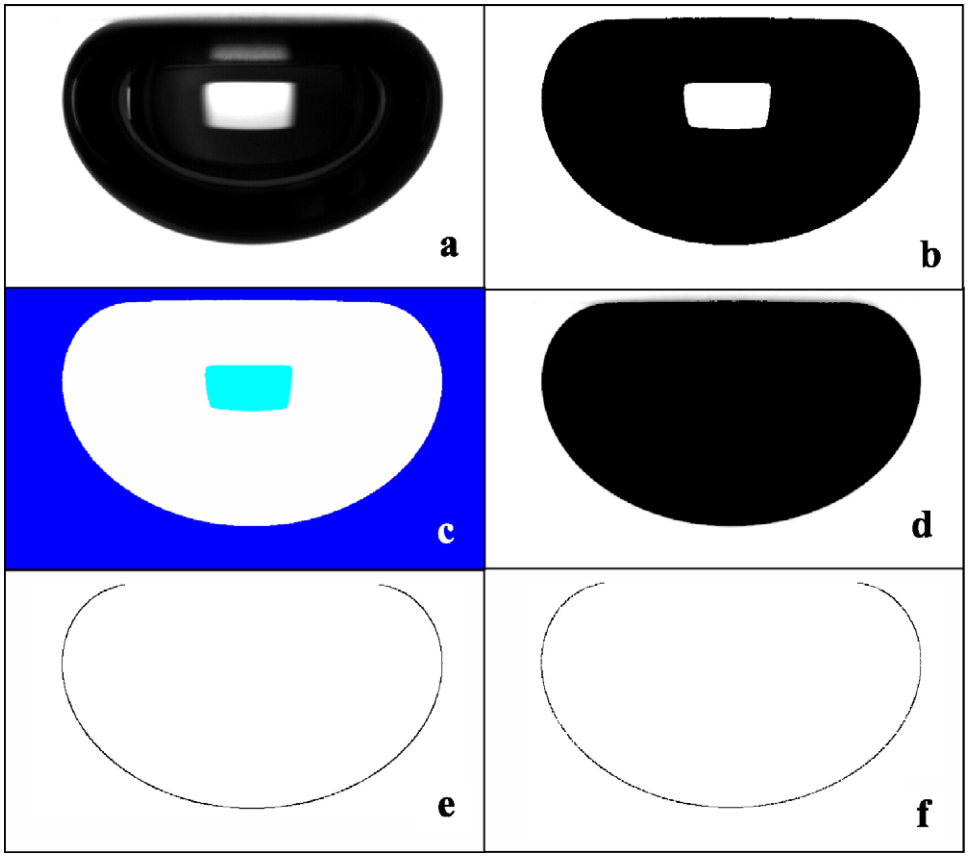

Fig. 4. Implementation of the image analysis in ADSA for a clean captive bubble image. (a) Original grayscale image showing a captive bubble in water; (b) binary image after Otsu's thresholding; (c) pseudocolor image showing 3 detected isolated components (each component is represented by one color) after component labeling; (d) grayscale image after removing isolated noise; (e) Canny detected edge (with pre-edge detection removal of the isolated noise); (f) ALFI-S smoothed edge (removing adhering noise).

bubble chamber is made of 1% agarose so that the entire bubble is clearly visible [30]. Fig. 4(b) shows the black-and-white image converted from the original grayscale image using Otsu's thresholding. Fig. 4(c) shows the pseudocolor image after component labeling. Here, each component is labeled by one color. Three components have been detected. They are: the background that contains 121 091 pixels, the bubble that contains 112 854 pixels, and the central highlight spot that contains 6695 pixels. Fig. 4(d) shows the grayscale image after removing the isolated noise due to the central highlight spot. It is noted that the contour of the bubble remains intact (see comparison between Fig. 4(a) and (d)). Fig. 4(e) and (f) shows the Canny detected edge from Fig. 4(d) and the final smoothed edge after ALFI-S, respectively. Both edges show smooth profiles, indicating the effectiveness of noise reduction. Surface tension calculated using ADSA from this smoothed bubble profile is 69.33 mJ/m^2, which is in a good agreement with the literature value of water at 37 °C, i.e., 70.05 mJ/m^2 [31]. It should be noted that the captive bubble image shown in Fig. 4(a) is only used to demonstrate the performance of the component labeling-based noise reduction rather than to illustrate the accuracy of ADSA. A higher accuracy of ADSA-CB has been demonstrated before [13]. Most likely, the value of 69.33 mJ/m^2 represents the actual surface tension of the bubble. To observe the exact surface tension of water requires considerable effort with respect to purity of the water and overall cleanliness. Such an effort was not needed for the purpose of the present illustration.

4.2. A captive bubble image with a noisy background

To further illustrate the effectiveness of the component labeling method, it was used to analyze a noisy image of a captive bubble in a mixture of 0.5 mg/mL BLES and 50 mg/mL PEG. Different from Fig. 4(a) and Fig. 5(a) was acquired from captive bubble equipment with a concave stainless steel ceiling without agar gel coating. Hence, the bubble together with the ceiling forms a complex in the digital image. The bubble can be

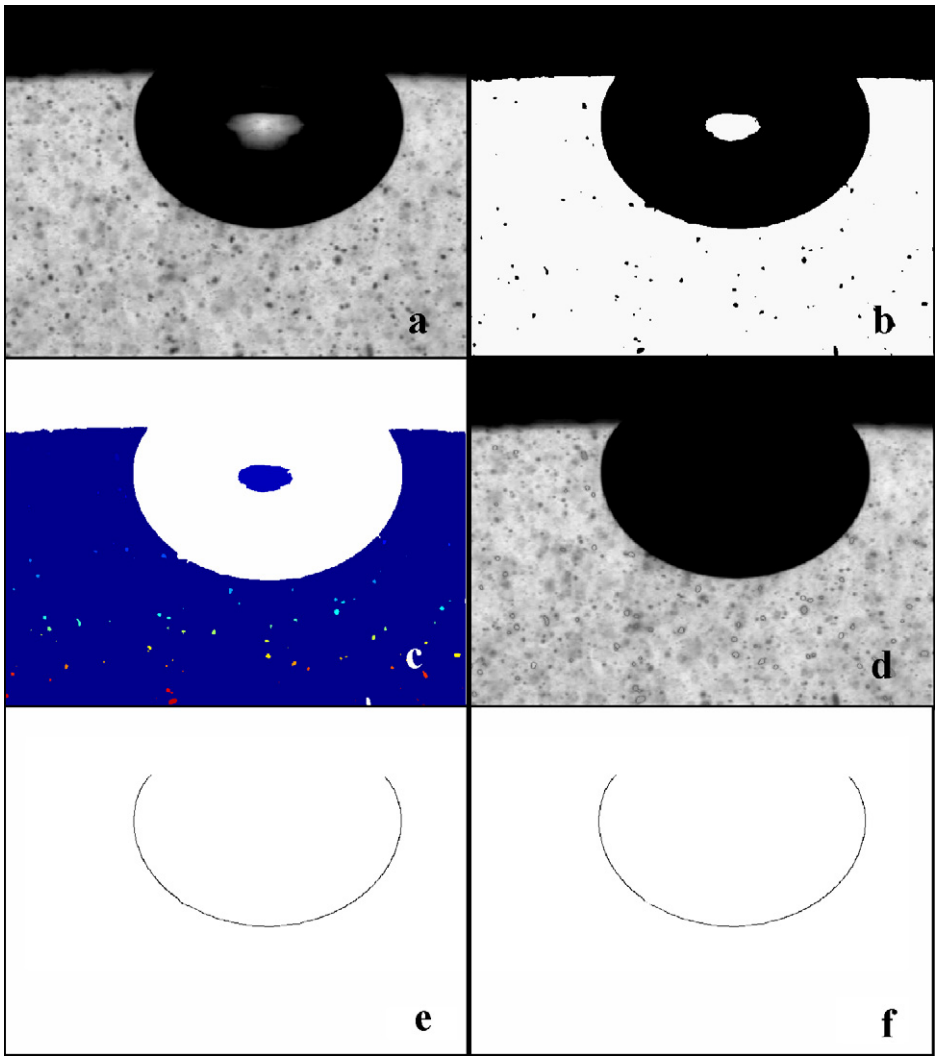

Fig. 5. Implementation of the image analysis in ADSA for a noisy captive bubble image. (a) Original grayscale image showing a captive bubble in the mixture of BLES and PEG; (b) binary image after Otsu's thresholding; (c) pseudocolor image showing 89 detected isolated components (each component is represented by one color) after component labeling; (d) grayscale image after removing isolated noise; (e) Canny detected edge (with pre-edge detection removal of the isolated noise); (f) ALFI-S smoothed edge (removing adhering noise).

easily separated from the ceiling later by setting up a rectangular working region in the image, as described before [13].

First, the original grayscale image (Fig. 5(a), resolution 480 × 640) is converted into a black-and-white image (Fig. 5(b)) using Otsu's thresholding. Second, the binary image is scanned for component labeling. Fig. 5(c) shows the pseudocolor image after component labeling. In total 89 components have been detected. The background accounts for the biggest component that consists of 177 324 pixels. The complex of the bubble and the ceiling accounts for the second biggest component, containing 126 658 pixels. The next is the highlight spot in the bubble center, containing 2118 pixels. The biggest isolated noise component due to surfactant aggregates contains 68 pixels and the smallest noise components consist of only 1 pixel. In addition to the suspending particles, other possible sources of the isolated noise (especially the 1-pixel noise) are uncertainties of the CCD sensor, fluctuation in the light intensity, and salt-and-pepper noise in signal transmission [32,33]. Although too small to be easily caught by the eyes, the component labeling method has successfully detected this 1-pixel noise, which proves that the method is highly sensitive and reliable.

After all the components have been labeled, the noise components are smoothed by replacing the original intensities of the noise pixels with the average of their neighbors'. In this way, the isolated noise "islands" in the background "ocean" are filled. The resultant image (Fig. 5(d)) shows a much smoother intensity transition in the original noise regions (see comparison between Fig. 5(a) and (d)). This less noisy image facilitates the subsequent edge detection. Fig. 5(e) shows the Canny detected bubble profile, which is very smooth. Fig. 5(f) shows the finally smoothed edge after ALFI-S. It is noted that the small bump on the Canny detected edge (i.e., adhering noise) is effectively removed. The surface tension value calculated from this smoothed edge is 23.67 mJ/m^2, which is consistent with data reported before [14].

5. Concluding remarks

A remaining obstacle for the fully automatic surface tension measurement was an effective image analysis scheme. This is especially importance for the measurement of turbid biofluids using a bubble method or interfacial tension measurement of turbid liquid–liquid systems. Such systems require an image analysis scheme robust against noise. It is desirable to extract unambiguous information on the characteristic parameters of a drop/bubble (e.g., height and diameter) or an undisturbed profile, even from a noisy background. It is also important to perform all these image analyses automatically because the surface tension of biofluids is typically highly dynamic, e.g., due to constant adsorption/desorption of the biomolecules. Hence, the analysis of a sequence of frames, corresponding to surface aging, should be conducted using only one set of user-specified input parameters without further human intervention, which makes automation a necessity of designing the methodologies.

A component labeling method has been developed to automatically remove the isolated noise from images for surface tension measurement. The component labeling procedure provides information on the localization of isolated objects in an image, including the background, the main foreground object (i.e., the drop/bubble), and the isolated noise. Hence, it is possible to smooth the detected noise (with known position) without compromising the profile of the drop/bubble. Therefore, the component labeling-based noise reduction method developed here acts as a selective low-pass filter which only smoothes the noise but does not blur the drop/bubble profile. This is a novel attempt to smooth an image in a pre-edge detection stage without compromising the accuracy of the subsequent edge detection. Demonstrations on both clean and noisy images show excellent results due to this additional noise reduction step. Compared with the previous noise reduction method by measuring edge cohesion, the component labeling method is more reliable. Fig. 2(c) and (d) shows the comparison of the detected edge from a fuzzy image using these two methods. It is clear that the component labeling method is able to effectively remove isolated noise and to retain a more complete edge.

It should also be noted that the component labeling method is a free-standing module for removing isolated noise. It is not indispensable; but, addition of this module would significantly increase the effectiveness and reliability of the image analysis. Although only the analysis of captive bubble images was demonstrated in this paper, application of the component labeling method would cover a broad range of problems mainly concerning region detection. For example, the component labeling method would be very suitable for the application of measuring very low contact angles of biotissues and surfaces with different coatings using axisymmetric drop shape analysis-diameter (ADSA-D) [34,35]. In such a context, the actual contour of a drop (image acquired from the top-view) is not of interest but rather the area or the equivalent diameter of the drop is needed. The component labeling method would be a match for such studies.

Combined with the Canny edge detector and ALFI-S for adhering noise reduction, the component labeling method developed here has greatly strengthened the effectiveness and reliability of the image analysis scheme used in ADSA. With the introduction of component labeling the image analysis scheme in ADSA is fully automatic and highly noise-resistant without significantly increasing the computational time (e.g., 1–2 s per captive bubble image using a PC with a 2.0 GHz CPU), which allows accurate surface tension measurement of turbid systems, such as lung surfactants. It should also be noted that the entire image analysis scheme is independent from ADSA. It can be used as a standard software package in combination with any other surface tension measurement methodology, for example, the widely used captive bubble surfactometer (CBS) in lung surfactant studies [29,36].

Acknowledgements

This work was supported by a grant from the Canadian Institutes of Health Research (MOP-38037) and an Open Fellowship from the University of Toronto to Y.Y.Z. We thank Dr. David Bjarneson of BLES Biochemicals, Inc. for his generous donation of the BLES samples. We also thank Dr. Ethan C. Smith

and Dr. Stephen B. Hall (Oregon Health & Science University) for kindly providing the image of a captive bubble in water used here as an illustration.

References

[1] A.W. Adamson, Physical Chemistry of Surfaces, 5th ed., Wiley, New York, 1990.
[2] A.W. Neumann, R.J. Good, Surface and Colloid Science, Plenum Press, New York, 1979.
[3] S. Lahooti, O.I. del Río, P. Cheng, A.W. Neumann, Axisymmetric drop shape analysis (ADSA), in: A.W. Neumann, J.K. Spelt (Eds.), Applied Surface Thermodynamics, Marcel Dekker, New York, 1996, pp. 441–507.
[4] Y. Rotenberg, L. Boruvka, A.W. Neumann, Determination of surface tension and contact angle from the shapes of axisymmetric fluid interfaces, J. Colloid Interface Sci. 93 (1983) 169–183.
[5] P. Cheng, D. Li, L. Boruvka, Y. Rotenberg, A.W. Neumann, Automation of axisymmetric drop shape analysis for measurements of interfacial tensions and contact angles, Colloids Surf. 43 (1990) 151–167.
[6] O.I. del Río, A.W. Neumann, Axisymmetric drop shape analysis: computational methods for the measurement of interfacial properties from the shape and dimensions of pendant and sessile drops, J. Colloid Interface Sci. 196 (1997) 136–147.
[7] D.B. Thiessen, K.F. Man, Surface tension measurement, in: J.G. Webster (Ed.), The Measurement, Instrumentation, and Sensors Handbook, CRC Press/IEEE Press, Boca Raton, 1999, pp. 31.1–31.13.
[8] Y.Y. Zuo, A.W. Neumann, Application of axisymmetric drop shape analysis (ADSA) to the study of biomolecules, in: P. Chen (Ed.), Molecular Interfacial Phenomena of Polymers and Biopolymers, Woodhead Publishing Ltd., Cambridge, UK, 2005, pp. 249–285.
[9] Y.Y. Zuo, A.W. Neumann, Pulmonary surfactant and its in vitro assessment using axisymmetric drop shape analysis (ADSA): a review, Tenside Surfact. Det. 42 (2005) 126–147.
[10] T. Kuhl, Y. Guo, J.L. Alderfer, A.D. Berman, D. Leckband, J. Israelachvili, S.W. Hui, Direct measurement of polyethylene glycol induced depletion attraction between lipid bilayers, Langmuir 12 (1996) 3003–3014.
[11] L.M.Y. Yu, J.J. Lu, I.W.Y. Chiu, K.S. Leung, Y.W. Chan, L. Zhang, Z. Policova, M.L. Hair, A.W. Neumann, Poly(ethylene glycol) enhances the surface activity of a pulmonary surfactant, Colloids Surf. B: Biointerfaces 36 (2004) 167–176.
[12] P. Cheng, A.W. Neumann, Computational evaluation of axisymmetric drop shape analysis-profile (ADSA-P), Colloids Surf. 62 (1992) 297–305.
[13] Y.Y. Zuo, M. Ding, A. Bateni, H. Hoorfar, A.W. Neumann, Improvement of interfacial tension measurement using a captive bubble in conjunction with axisymmetric drop shape analysis (ADSA), Colloids Surf. A: Physicochem. Eng. Aspects 250 (2004) 233–246.
[14] Y.Y. Zuo, M. Ding, D. Li, A.W. Neumann, Further development of axisymmetric drop shape analysis-captive bubble (ADSA-CB) for pulmonary surfactant related studies, Biochim. Biophys. Acta 1675 (2004) 12–20.
[15] A.K. Jain, Fundamentals of Digital Image Processing, Prentice-Hall, New York, 1989.
[16] M. Seul, L. O'Gorman, M.J. Sammom, Practical Algorithms for Image Analysis, Description, Examples and Code, Cambridge University Press, New York, 1999.
[17] F. Chang, C.J. Chen, C.J. Lu, A linear-time component-labeling algorithm using contour tracing technique, Comput. Vis. Image Und. 93 (2004) 206–220.
[18] K. Suzuki, I. Horiba, N. Sugie, Linear-time connected-component labeling based on sequential local operations, Comput. Vis. Image Und. 89 (2003) 1–23.
[19] Y. Yang, D. Zhang, A novel line scan clustering algorithm for identifying connected components in digital images, Image Vis. Comput. 21 (2003) 459–472.
[20] J. Rodriguez, D. Ayala, Fast neighbourhood operations for images and volume data sets, Comput. Graph. 27 (2003) 931–942.
[21] V. Khanna, P. Gupta, C.J. Hwang, Finding connected components in digital images by aggressive reuse of labels, Image Vis. Comput. 20 (2002) 557–568.
[22] P. Bhattacharya, Connected component labeling for binary images on a reconfigurable mesh architectures, J. Syst. Architect. 42 (4) (1996) 309–313.
[23] M.B. Dillencourt, H. Samet, M. Tamminen, A general approach to connected-component labeling for arbitrary image representations, J. Assoc. Comput. Mach. 39 (1992) 253–280.
[24] R. Lumia, L. Shapiro, O. Zungia, A new connected components algorithm for virtual memory computers, Comput. Vis. Graph. Image Process. 22 (1983) 230–287.
[25] A. Rosenfeld, P. Pfaltz, Sequential operations in digital picture processing, J. Assoc. Comput. Mach. 13 (1966) 471–494.
[26] R. Jain, R. Kasturi, B.G. Schunck, Machine Vision, McGraw-Hill, New York, 1995.
[27] S.E. Umbaugh, Computer Imaging: Digital Image Analysis and Processing, CRC Press, Boca Raton, 2005.
[28] N. Otsu, A threshold selection method from gray-level histogram, IEEE Trans. Syst. Man Cybernet. 9 (1979) 62–66.
[29] S. Schürch, H. Bachofen, J. Goerke, F. Possmayer, A captive bubble method reproduces the in situ behavior of lung surfactant monolayers, J. Appl. Physiol. 67 (1989) 2389–2396.
[30] J.M. Crane, G. Putz, S.B. Hall, Persistence of phase coexistence in disaturated phosphatidylcholine monolayers at high surface pressures, Biophys. J. 77 (1999) 3134–3143.
[31] N.B. Vargaftik, B.N. Volkov, L.D. Voljak, International tables of the surface tension of water, J. Phys. Chem. Ref. Data 12 (1983) 817–820.
[32] J.A. Holgado-Terriza, J.F. Gómez-Lopera, P.L. Luque-Escamilla, C. Atae-Allah, M.A. Cabrerizo-Vilchez, Measurement of ultralow interfacial tension with ADSA using an entropic edge-detector, Colloids Surf. A: Physicochem. Eng. Aspects 156 (1999) 579–586.
[33] C. Atae-Allah, M.A. Cabrerizo-Vilchez, J.F. Gómez-Lopera, J.A. Holgado-Terriza, R. Román-Roldán, P.L. Luque-Escamilla, Measurement of surface tension and contact angle using entropic edge detection, Meas. Sci. Technol. 12 (2001) 288–298.
[34] J.M. Alvarez, A. Amirfazli, A.W. Neumann, Automation of the axisymmetric drop shape analysis-diameter for contact angle measurements, Colloids Surf. A: Physicochem. Eng. Aspects 156 (1999) 163–176.
[35] M.A. Rodríguez-Valverde, M.A. Cabrerizo-Vílchez, P. Rosales-López, A. Páez-Dueñas, R. Hidalgo-Álvarez, Contact angle measurements on two (wood and stone) non-ideal surfaces, Colloids Surf. A: Physicochem. Eng. Aspects 206 (2002) 485–495.
[36] W.M. Schoel, S. Schürch, J. Goerke, The captive bubble method for the evaluation of pulmonary surfactant: surface tension, area, and volume calculation, Biochim. Biophys. Acta 1200 (1994) 281–290.